Chapter 9
Discrete Model for Plate Bending

9.1 Beam Model

In Chapter 8 we discussed an approximation for trusses. The elastic deformations were lumped in springs. We may apply a similar model to beams in bending as a first step to a discrete model for plate bending. A rigid element that has rotational springs at its ends replaces a beam element of length a. This model is depicted in Figure 9.1. The rotational spring is considered to be composed of two parallel springs, for the compression and tension zones, respectively. The rotational rigidity at each end is D. It is required that the beam-ends in both the model and the actual beam have the same rotation e for a constant moment M. This requirement is met if $D = 2EI/a$. When two beam elements are linked together, the two rotational end springs are connected in series. The rigidity of the resulting rotational spring is $D = EI/a$.

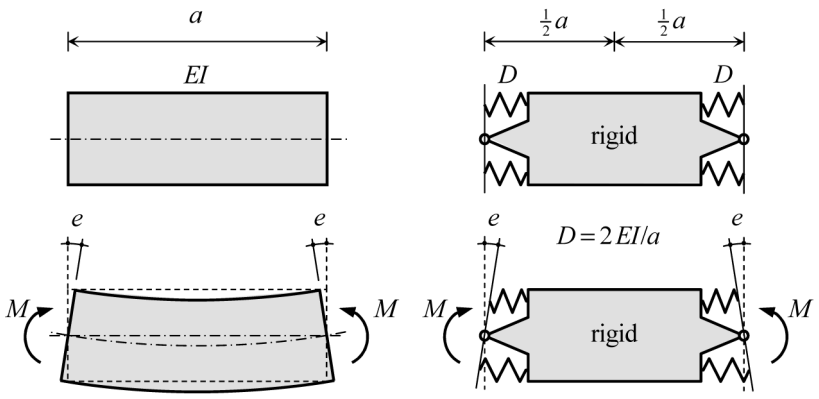

Figure 9.1 Discrete bending model for beam.

J. Blaauwendraad, *Plates and FEM: Surprises and Pitfalls*, Solid Mechanics and Its Applications 171, DOI 10.1007/978-90-481-3596-7_9,

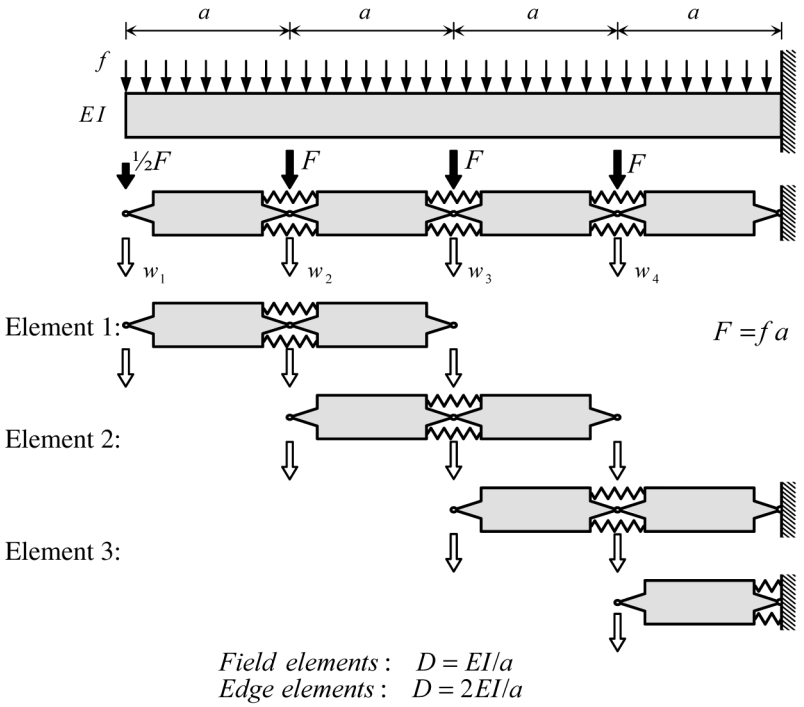

Figure 9.2 Modelling of a cantilever beam.

Figure 9.2 shows a cantilever beam modelled by four beam parts with length a. The homogeneous load is lumped at the hinges between the four sections. The deflections of the hinges are the unknowns. The structure is considered to be an assembly of four discrete elements and to have four degrees of freedom. The elements 1, 2, and 3 each have three degrees of freedom, element 4 only has one. This latter element is used at the clamped end. It need also to be used in a line of symmetry. Then the element has two degrees of freedom. Naturally, this element may occur with the rotational spring at the other end as well. First, the different stiffness matrices of the two element types are derived. The element types will be named *field element* and *edge element* respectively. The stiffness matrices for a field element with nodes i, j, k and an edge element with nodes i, j are respectively

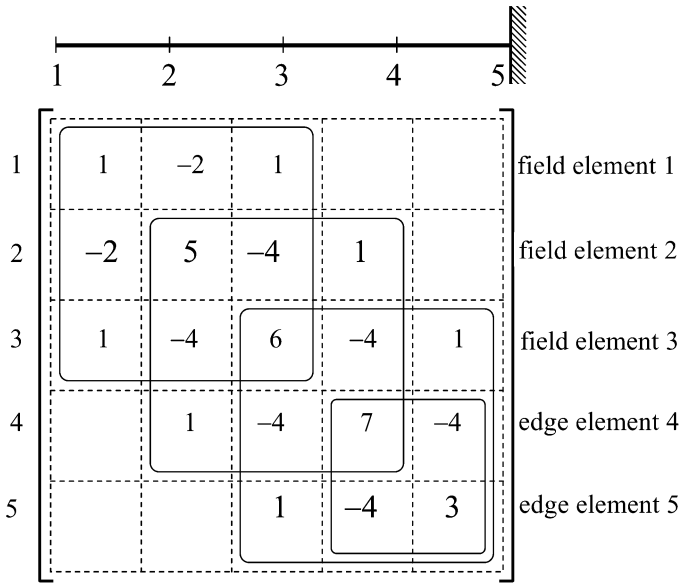

Figure 9.3 Composition of the global stiffness matrix.

$$\begin{Bmatrix} F_i \\ F_j \\ F_k \end{Bmatrix} = \frac{D}{a^2} \begin{bmatrix} 1 & -2 & 1 \\ -2 & 4 & -2 \\ 1 & -2 & 1 \end{bmatrix} \begin{Bmatrix} w_i \\ w_j \\ w_k \end{Bmatrix} \qquad (9.1)$$

$$\begin{Bmatrix} F_i \\ F_j \end{Bmatrix} = \frac{D}{a^2} \begin{bmatrix} 1 & -1 \\ -1 & 1 \end{bmatrix} \begin{Bmatrix} w_i \\ w_j \end{Bmatrix}$$

The stiffness matrix of the cantilever beam structure is an assembly of three field elements and one edge element. The result is shown in Figure 9.3. The matrix needs to be multiplied by EI/a^3. As is seen in the figure, the displacements are not yet constrained. If displacements are prescribed, corresponding rows and columns are omitted. Figure 9.4 shows a number of possibilities. The third row of the stiffness matrix is complete; that is to say, there is no influence of the boundaries on the coefficients of this row. If we use a finer mesh in the model, then the global stiffness matrix would contain more of these complete rows. Apart from the multiplication factor EI/a^3, the scheme shown in Figure 9.5 applies for nodes not affected by any edge conditions.

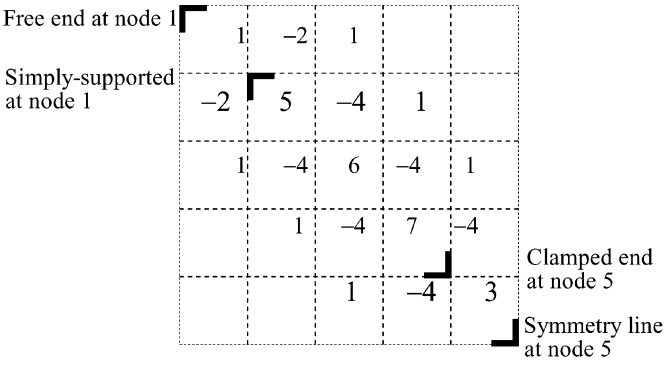

Figure 9.4 Effect of various boundary conditions.

Figure 9.5 Scheme for a complete field row.

9.1.1 Example. Cantilever Beam

The set of equations has been solved for the cantilever beam of Figure 9.6. The nodal force is $F = fa$. The matrix equation reads:

$$\frac{EI}{a^3}\begin{bmatrix} 1 & -2 & 1 & & \\ -2 & 5 & -4 & 1 & \\ 1 & -4 & 6 & -4 & 1 \\ & 1 & -4 & 7 & -4 \\ & & 1 & -4 & 3 \end{bmatrix} \begin{Bmatrix} w_1 \\ w_2 \\ w_3 \\ w_4 \\ w_5 \end{Bmatrix} = \begin{Bmatrix} \frac{1}{2}fa \\ fa \\ fa \\ fa \\ \frac{1}{2}fa + R \end{Bmatrix} \tag{9.2}$$

The dotted lines hold for the matrix equation in which boundary conditions have not yet been introduced, the full lines after accounting for the boundary conditions. The solution of the set of equations is

$$\{w_1 \;\; w_2 \;\; w_3 \;\; w_4\} \;\; w_5\} = \frac{a^4 f}{EI}\{34 \;\; 23 \;\; 12\tfrac{1}{2} \;\; 4\} \;\; 0\} \tag{9.3}$$

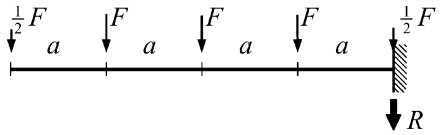

Figure 9.6 Cantilever beam with four elements.

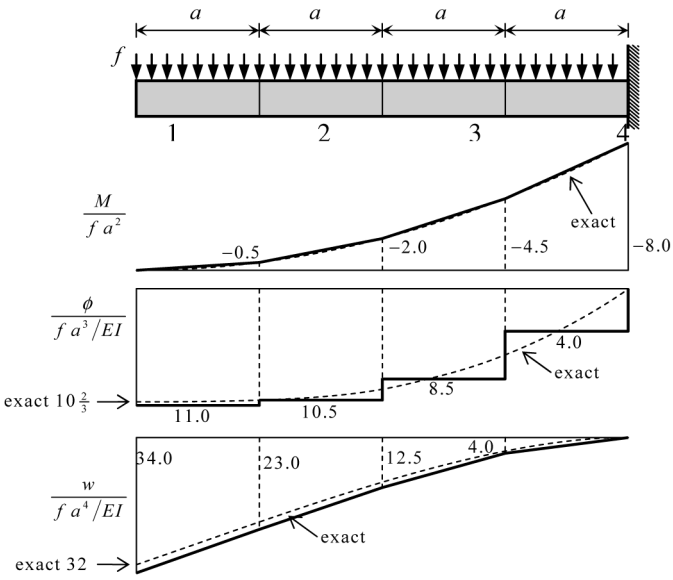

Figure 9.7 Cantilever results for exact solution and approximation

The support reaction, calculated from the fifth row in Eq. (9.2), is $R = -4fa$. The moments are determined from the spring equations

$$\begin{aligned} M &= \frac{EI}{a^2}(-w_i + 2w_j - w_k) \quad \textit{Field element} \\ M &= 2\frac{EI}{a^2}(w_j - w_i) \qquad\quad \textit{Edge element} \end{aligned} \tag{9.4}$$

The results are depicted in Figure 9.7. Even this course mesh and simple elements give a good approximate result.

Same pattern of coefficients in Finite Difference Method

When the classical Finite Difference Method (FDM) is applied, the differential equation $EI\, d^4w/dx^4 = f$ is replaced by a set of algebraic equations, one for each node. The FDM-equation related to node 3, which is not influenced by the boundary conditions, is exactly the same as the third row in the above matrix equation. So, the scheme of Figure 9.5 is both the scheme in FDM and the present discrete model. The rotational spring method is not restricted to equal element dimensions

and constant bending rigidity EI for all elements. Serial linking of different spring stiffness is allowed.

9.2 Plate Bending Model

The spring model for bending of the previous section is a building block for the discrete plate bending model, just as the truss model was for the discrete membrane model. We consider a rectangular plate element of length a and width b, subjected to a homogeneously distributed load p. The plate thickness is t, Young's modulus is E, and Poisson's ratio is zero. The relation between the moments and curvatures is

$$\begin{Bmatrix} m_{xx} \\ m_{yy} \\ m_{xy} \end{Bmatrix} = D \begin{bmatrix} 1 & 0 & 0 \\ 0 & 1 & 0 \\ 0 & 0 & \frac{1}{2} \end{bmatrix} \begin{Bmatrix} \kappa_{xx} \\ \kappa_{yy} \\ \rho_{xy} \end{Bmatrix} \tag{9.5}$$

Here the *plate flexural rigidity* is $D = Et^3/12$. The rigidity matrix is a diagonal matrix, therefore bending in the x-direction and y-direction are independent of each other. Torsion is another independent transfer mechanism.

The bending behaviour in the x- and the y-direction is modelled with the spring elements derived in Section 9.1. Thus an orthogonal grid of beams is obtained. To account for twisting moments, torsion panels are inserted in the grid in the same way as shear panels were in the membrane model. From Section 5.2 we know that a field of constant m_{xy} can exist if the panel is loaded by two pairs of equilibrating corner point loads occur, and that the edges remain straight. On the basis of this knowledge a torsion panel can be derived with four degrees of freedom as shown in Figure 9.8. The stiffness

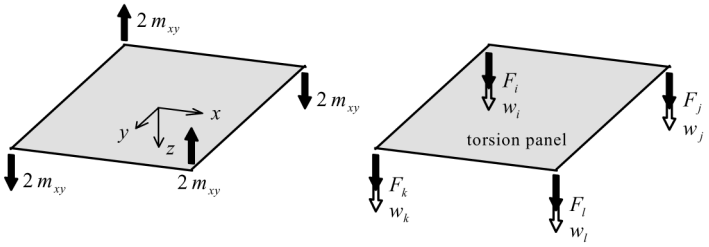

Figure 9.8 Loading for positive twisting moment. Left physical reality, right stiffness method.

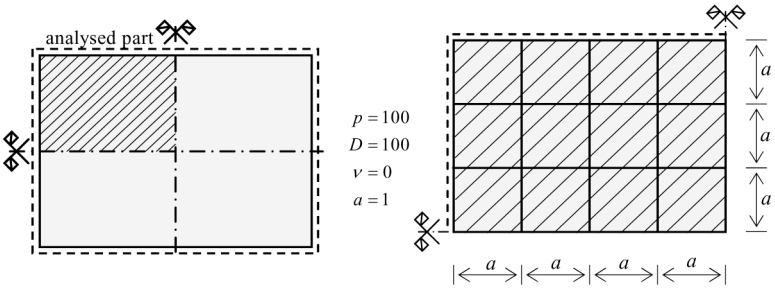

Figure 9.9 Uniformly loaded simply-supported rectangular plate.

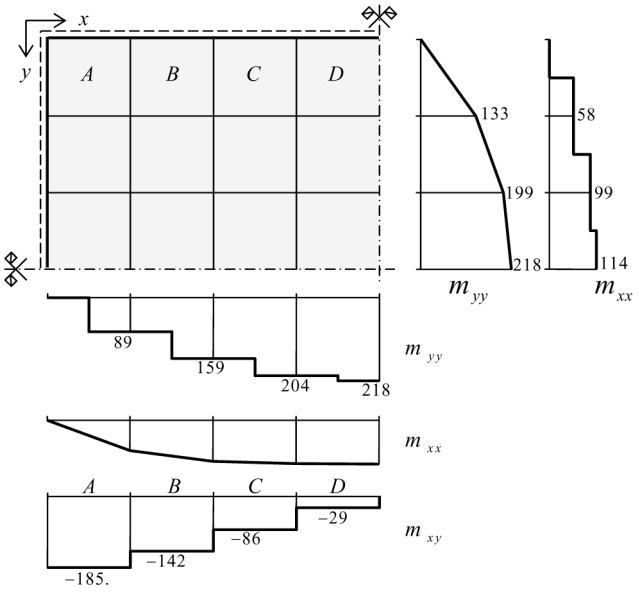

Figure 9.10 Moment distributions in the slab.

matrix of this panel is

$$\begin{Bmatrix} F_i \\ F_j \\ F_k \\ F_l \end{Bmatrix} = \frac{D}{a\,b} \begin{bmatrix} 2 & -2 & -2 & 2 \\ -2 & 2 & 2 & -2 \\ -2 & 2 & 2 & -2 \\ 2 & -2 & -2 & 2 \end{bmatrix} \begin{Bmatrix} w_i \\ w_j \\ w_k \\ w_l \end{Bmatrix} \tag{9.6}$$

Any plate that may be considered a composition of rectangular plate parts can now be modelled with spring elements and torsion panels.

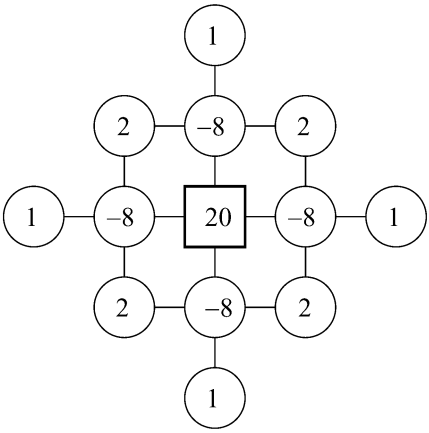

Figure 9.11 Scheme for both FDM and discrete model.

9.2.1 Example 1. Rectangular Simply-Supported Plate

We will perform the discrete analysis for the example of Figure 9.9. For reasons of symmetry only one quarter of the plate needs to be modelled. The computational result is presented in Figure 9.10. As was seen earlier for the normal forces in the membrane solution, we again obtain a continuous distribution for the bending moments in the one direction and a discontinuous one in the other. Like the shear forces in the membrane solution, now the twisting moment is discontinuous.

Advantage of discrete model

In the Finite Difference Method (FDM) the bi-harmonic differential equation is replaced by a set of linear algebraic equations, one for each mesh node. For nodes which are at sufficient distance from the edge the scheme of coefficients is shown in Figure 9.11. The discrete model with flexural springs and torsion panels leads to the same result. The advantage of the discrete modelling is the ease of handling boundary conditions, discontinuities in thickness, and non-square meshes.

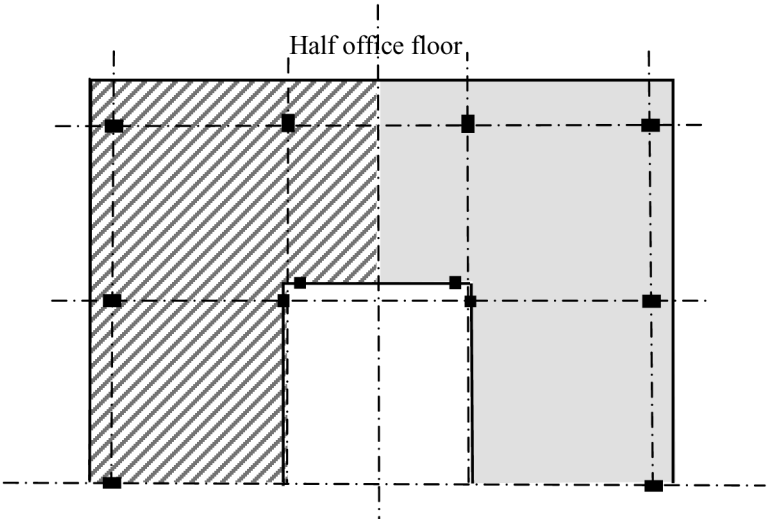

Figure 9.12 Application of discrete model to office building floor.

9.2.2 Example 2. Lift-Slab in Office Building

The model was in use in the 1960s for the analysis of viaducts and floor slabs in office buildings. An example is the floor of the office building in Figure 9.12 as built at Amsterdam Airport. The contractor cast and cured all floors at ground level around a tall central shaft (not shown in Figure 9.12), and then lifted them in place. Therefore they are not clamped to the central shaft, but just connected at discrete points. The hatched quarter of the floor has been considered in the analysis. The bending moments for two directions are shown in Figure 9.13.

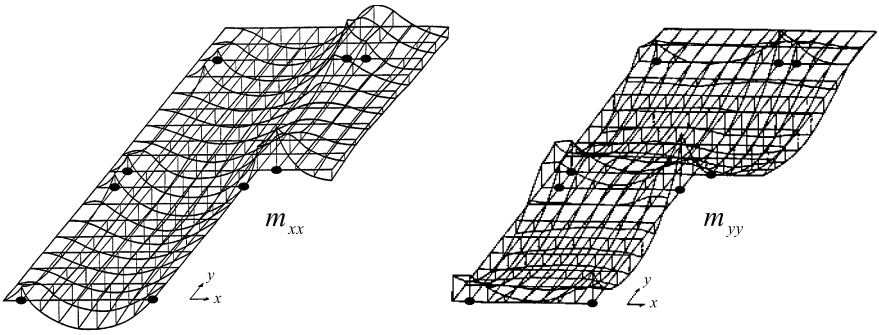

Figure 9.13 Bending moments in quarter of floor slab.

9.3 Didactical Model for Simply-Supported Plate

The discrete model is no longer in use since Finite Element Analysis has replaced it, however it still has great didactical value. This value is illustrated for the simply-supported plate, subjected to a two-way sine load, the exact solution of which we discussed in Section 5.3. Here we recall the most important results of the exact analysis. The deflection w and bending moments m_{xx} and m_{yy} have double-sine distributions, with a maximum in the centre of the plate. The twisting moment has a double-cosine distribution with a value zero in the horizontal and vertical line of symmetry. The maximum value occurs at the four corners. The shear forces v_x and v_y have sine-shaped distributions in the one direction and cosine-shaped in the other. Their maximum value appears at the edges. The distributed support reactions f (positive if directed downward) along the four edges are sine-shaped with a maximum value halfway along the edges. The various maxima are, apart of the sign

$$w = \frac{\hat{p}\, l^4}{4\pi^4 D}, \quad m_{xx} = m_{yy} = \frac{\hat{p}\, l^2}{4\pi^2}, \quad m_{xy} = \frac{\hat{p}\, l^2}{4\pi^2}$$
$$v_x = \frac{1}{2\pi}\hat{p}\, l, \quad v_y = \frac{1}{2\pi}\hat{p}\, l, \quad f = -\frac{3}{4\pi}\hat{p}\, l \tag{9.7}$$

where $\hat{p}$ is the maximum value of the load and D is the plate stiffness. The support reaction is 50% larger in absolute value than the maximum shear force at the edge. The negative sign means that it concerns a compressive support reaction in the opposite direction to the load p. Finally it was found that four balancing concentrated corner tensile support reactions R occur with the value

$$R = \frac{1}{2}\,\hat{p}\, l^2/\pi^2 \tag{9.8}$$

We now start to explain the discrete model. The coarsest mesh possible is a two-by-two grid with one central node; there is just one degree of freedom. However, a three-by-three mesh leads also to one degree of freedom; There are four free nodes in the plate, but they all have the same displacement. This finer mesh will produce more information, and therefore is chosen. The square plate has edges of length l which are divided in three equal parts a. Figure 9.14 shows the applicable discrete model of four beams, two in each direction.

In a three-by-three grid we need in general nine torsion panels, but in our case five of them occur on lines of symmetry and therefore will have zero twist. So, just the four corner panels need be entered in the analysis,

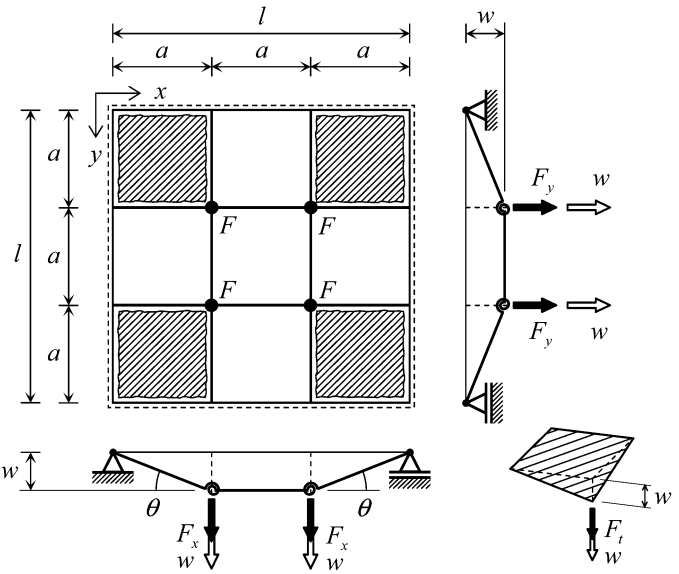

Figure 9.14 Elementary spring-panel model for a square plate.

which confirms the importance of torsion in the corners. The two-way sine load is replaced by four point loads F each pa^2. We restrict the analysis to a zero Poisson's ratio. The model is very simple. The load F at each free point is carried by three elements, a beam in the x-direction, a beam in the y-direction and a torsion panel. The three contributions are F_x, F_y and F_t, respectively. They are derived in an elementary way on the basis of the properties of the spring model and torsion model

$$F_x = \frac{D\,w}{a^2}, \quad F_y = \frac{D\,w}{a^2}, \quad F_t = 2\,\frac{D\,w}{a^2} \tag{9.9}$$

The three contributions are related to the same displacement and are linked in parallel. Therefore they can be summed, which leads to the relation between the displacement w and the load F

$$F_x + F_t + F_y = F, \quad \frac{D}{a^2}\,(1+2+1)\,w = F, \quad w = \frac{Fa^2}{4D} \tag{9.10}$$

Clearly

$$F_x = \frac{1}{4}F, \quad F_y = \frac{1}{4}F, \quad F_t = \frac{1}{2}F \tag{9.11}$$

This very elementary model effectively confirms what was seen earlier after solving the bi-harmonic equation for a double-sine load in Section 5.3. The

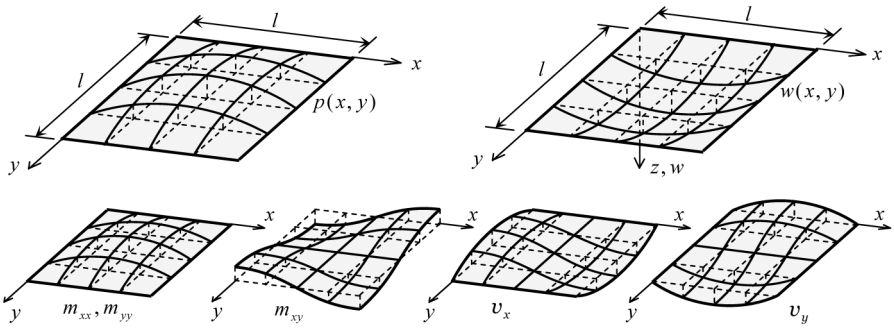

Figure 9.15 Exact results for a two-way sine load.

torsion in the plate carries half the load, and the deflection is a quarter of the value that occurs if one beam had to transfer all the load F. The bending moment at the position of the rotational springs, the twisting moment in the panels, and the shear forces midway between the two nodes become

$$m_{xx} = m_{yy} = m_{xy} = \frac{1}{4}F, \quad v_x = v_y = \frac{1}{2}\frac{F}{a} \tag{9.12}$$

As we found for zero Poisson's ratio in the exact solution, the maximum torsion moment is equal to the maximum bending moment. Figure 9.16 compares the results of the discrete moments to the outcome of the exact analysis for a number of sections over the plate. Figure 9.17 does the same for the shear force and support reaction. Finally, we can calculate the reaction forces in the edge and corner nodes. The simple model leads to $R_{\text{corner}} = \frac{1}{2}F$, $R_{\text{edge}} = -\frac{3}{4}F$. Figure 9.18 presents an overview of these boundary forces. The distributed support reaction $f = R_{\text{edge}}/a = -\frac{3}{4}F/a$ is again 50% larger in absolute value than the shear force v_x. For vertical equilibrium of the total plate it is required that $4R_{\text{corner}} + 8R_{\text{edge}} + 4F = 0$. This is indeed satisfied: $4(\frac{1}{2}F) + 8(-\frac{3}{4}F) + 4F = 0$. All the results that were seen in the solution of the bi-harmonic equation reappear in this elementary model.

Comparison

The results of the discrete model are compared to the exact solution of the square simply supported plate subjected to a double-sine load. Table 9.1 lists the maximum occurring values of the displacement w, the moments m, the shear force v, the distributed support reaction f and the concentrated corner reaction R_{corner} is given. The results of the discrete model and the exact so-

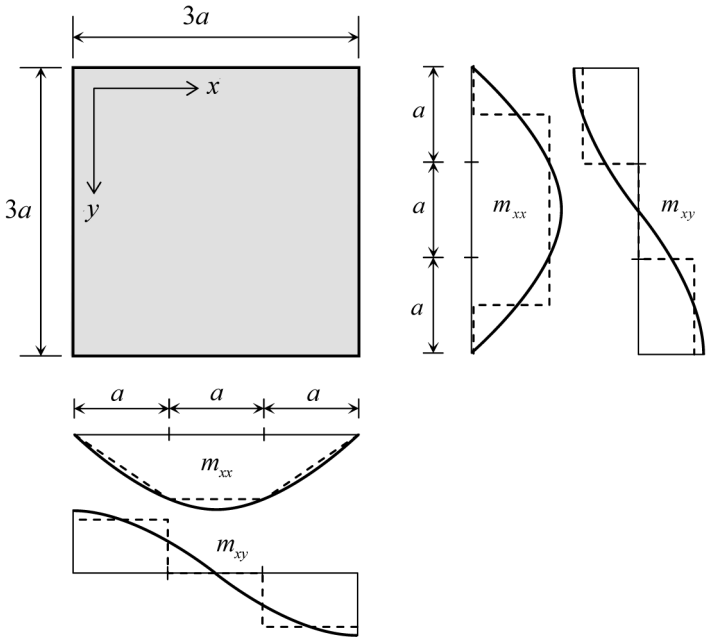

Figure 9.16 Comparison between discrete model and exact solution for moments.

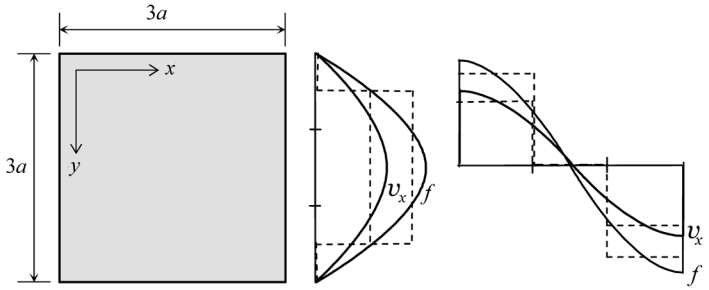

Figure 9.17 Comparison between discrete model and exact solution for shear force and support reaction.

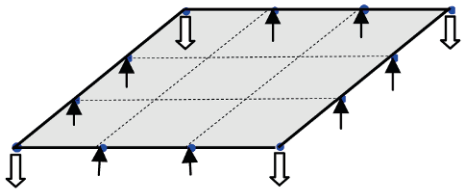

Figure 9.18 Distribution of support reactions.

Table 9.1 Comparison of discrete model with exact values for two-way sine load.

	Exact values divided by pl^2/π^2	Values for discrete model divided by $F = pl^2/9$
w	$l^2/(4\pi^2 D)$	$l^2/(4 * 9D)$
m	1/4	1/4
v	$\pi/2l$	$3/2l$
f	$-3\pi/4$	$-3 * 3/4$
R_{corner}	1/2	1/2

lution are very close to each other. The simple model accurately shows the main aspects in the force transfer of a simply-supported plate:

1. Maximum bending moments m_{xx} and m_{yy} occur at the centre of the plate.
2. Maximum twisting moments m_{xy} occur at the corners, and have the same magnitude as the bending moments.
3. The distributed support reactions are 50% larger than the shear forces.
4. Lumped tensile corner support reactions are twice the size of the twisting moments.

9.4 Discrete Model for Plate on Flexible Edge Beams

In the previous section we modelled the simply-supported plate which had been discussed in Section 5.3 for a two-way sine load. In Section 5.4 we considered another interesting case, a flexible edge beam, which leads to a twist-less plate, at that time for a homogeneously distributed load. Because the two cases have different loads and different boundary conditions, we had to study them with different displacement fields. With the discrete model we can study both cases in one model for the same load. We will do so for the square model of Figure 9.14 and a homogeneously distributed load p.

The new model is shown in Figure 9.19. The grid consists of four beams in the x-direction, four in the y-direction, and four torsion panels. The beams inside the plate represent a plate strip of width a. The beams at the position of the edge represent the actual applied edge beam plus a plate strip of width $\frac{1}{2}a$. Because the edges can deflect, an additional degree of freedom must be introduced. We call the displacement of each inner node w_1 and of each edge node w_2. Now the stiffness matrix of the plate has two rows and two columns.

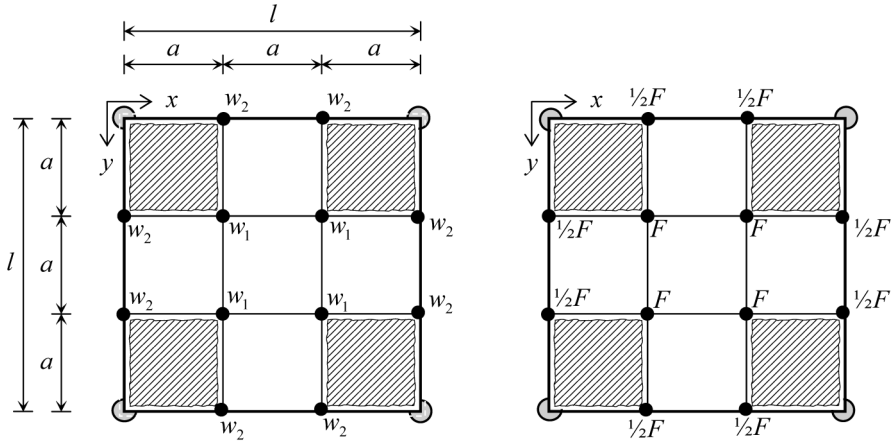

Figure 9.19 Discrete model for plate with flexible edge beams.

We introduce the edge beam flexural rigidity $EI = \lambda(\frac{1}{2}lD)$, where $l = 3a$ is the length of the plate edge and D the plate flexural rigidity; the parameter λ relates the beam rigidity to the rigidity of the half plate width. Now we obtain, on the basis of the properties of the rotational spring elements and torsion panel, the following matrix equation

$$\frac{D}{a^2}\begin{bmatrix} 4 & -6 \\ -6 & 11+3\lambda \end{bmatrix}\begin{Bmatrix} w_1 \\ w_2 \end{Bmatrix} = F\begin{Bmatrix} 1 \\ 1 \end{Bmatrix} \tag{9.13}$$

The force F is equal to pa^2. We found the solution of this matrix equation for three different values of the parameter λ

$$\begin{aligned} \lambda = \infty \;&\rightarrow\; w_1 = \frac{1}{4}\frac{Fa^3}{D}, \quad w_2 = 0 \\ \lambda = 1 \;&\rightarrow\; w_1 = \frac{Fa^3}{D}, \quad w_2 = \frac{1}{2}\frac{Fa^3}{D} \\ \lambda = 0 \;&\rightarrow\; w_1 = \frac{17}{8}\frac{Fa^3}{D}, \quad w_2 = \frac{Fa^3}{D} \end{aligned} \tag{9.14}$$

The computation of the bending and torsion moments from these displacements is a straight-forward procedure. The bending moment along a section at mid-span and the torsion moment along the edge are presented in Figure 9.20. The case of infinite large λ corresponds to the simply-supported case. The same solution is obtained as in the previous Section. The twisting moments and the bending moments are equal. For

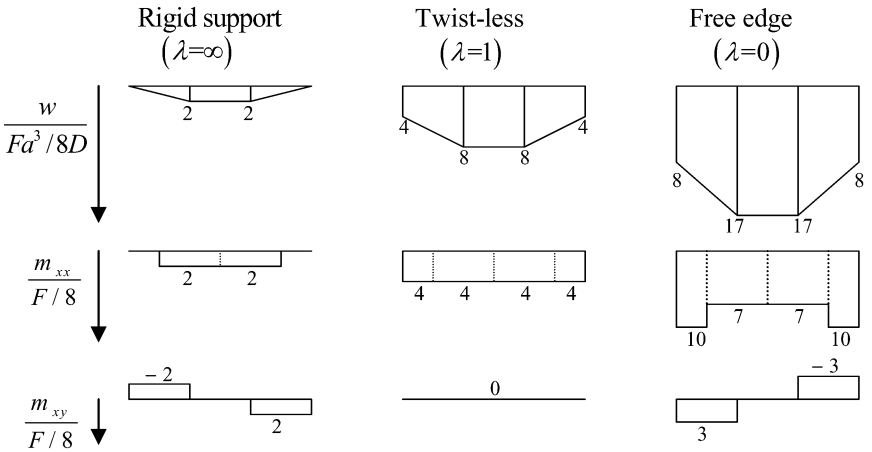

Figure 9.20 Results for different edge beam stiffness.

$\lambda = 1$, the plate becomes twist-less; all twisting moments are zero; the edge beam has the same stiffness as the half plate width. For $\lambda = 0$ the plate has free edges and is supported just by four compressive point loads in the corners. Twisting moments occur, but they have an opposite sign compared to the simply-supported plate. There, the corner reaction was tensile, here it is compressive. When λ decreases from infinity to zero, we see the twisting moments switch sign, and notice a substantial increase of the bending moments. In Figure 9.20, note the large increase of deflection, the substantial increase in the bending moments, and the switch in sign of the twisting moments.

The total bending moment over the full width of the plate at mid-span due to the load is $3Fa$, which is equal to $pl^3/9$. Part of this moment is carried by the plate and part by the edge beams. For the three considered cases of rigid supports, twist-less plate and free edges, the plate part is 1/6, 1/2 and 1, respectively. Two edge beams account for the remaining part, 5/6, 1/2 and 0, respectively. The moment in each edge beam becomes $pl^3/21.6$, $pl^3/32$ and 0, respectively.

It is interesting to compare these values to those arising from the practical approach of structural engineers and recommendations in some codes of practice, in which the load is supposed to flow to the beams as depicted in Figure 9.21, referred to as *envelope approach*. For a square plate this leads to a distributed beam load of triangular shape with maximum value $pl/2$ at mid-span. In its turn, this load leads to a bending moment $pl^3/24$, which is

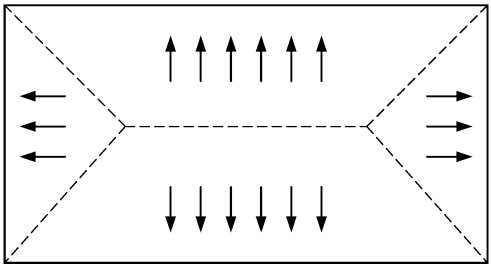

Figure 9.21 Loading of edge beams in 'envelope' approach.

10% too small, compared to the exact value $pl^3/21.6$ for an infinite rigid beam. For flexible edge beams in a twist-less plate with exact moment value $pl^3/32$, it is too large. Then the envelope approach overestimates the moment by 50%.

If a structural engineer is detailing flexible edge beams on the basis of the envelope approach, the reinforcement in the plate itself may be too weak. Even though safety may not be affected, there may be severe cracking in practice.

9.5 Message of the Chapter

- Plate bending can be modeled by a grid of beams filled in by torsion panels. The beams in their turn can be modeled by rotational spring elements.
- The spring-panel model elegantly shows that the central part of a square simply-supported plate under distributed loading is dominated by bending and the corner parts by torsion, and that the maximum bending moment is equal to the maximum twisting moment for zero Poisson's ratio.
- Equations in the global stiffness matrix are similar to those in the classical Finite Difference Method.

- The effect of edge beams can be shown by a simple hand calculation with two degrees of freedom. Very stiff edge beams and very flexible edge beams both lead to twisting moments in the corner regions of the plate, however of opposite sign. For an in between edge beam stiffness the plate is perfectly twist-less.

- For infinitely rigid edge beams, the engineering envelope approach to calculate the maximum edge beam moment is 10% too optimistic. It is 50% too pessimistic for flexible beams with a torsion-less plate.